Dynamic universality for Z_2 and Z_3 lattice gauge theories at finite temperature

R. C. Brower
Physics Department and Department of Electrical, Computer and Systems Engineering, Boston University, 590 Commonwealth Avenue, Boston, Massachusetts 02215

Suzhou Huang
Physics Department, Boston University, 590 Commonwealth Avenue, Boston, Massachusetts 02215 and Department of Physics FM-15, University of Washington, Seattle, Washington 98195

(Received 29 March 1991)

Swendsen-Wang random surface dynamics for Z_2 and Z_3 gauge theories in $2+1$ dimensions is applied to the finite-temperature deconfining transition, and the static universality conjecture of Svetitsky and Yaffe is extended to the exponent z for critical dynamics. Our new dynamic universality conjecture ($z_{\rm RS}^{d+1}=z_{\rm SW}^{d}$) is supported both by a qualitative argument and by numerical simulations that show that the dynamic critical exponents for $(2+1)$-dimensional gauge theories (logarithmic or $z_{\rm RS}<0.3\pm0.1$ and 0.53 ± 0.03 for Z_2 and Z_3, respectively) are consistent with the values for the two-dimensional Ising-Potts models (logarithmic or $z_{\rm SW}=0.20$–0.27 and 0.55 ± 0.03 for Z_2 and Z_3, respectively) at the finite-temperature transition.

I. INTRODUCTION

Critical slowing down is expected to become a progressively more serious problem for lattice-gauge-theory simulations of QCD as we approach the continuum limit. One promising new method to reduce critical slowing down is provided by generalizations of the Swendsen-Wang cluster dynamics [1]. In the case of spin models, cluster algorithms for Potts models and their extension to continuum spin (or Higgs) systems by Brower and Tamayo [2] and Wolff [3] have proven that these nonlocal methods do accelerate Monte Carlo equilibration by several orders of magnitude on lattices with correlation lengths in the range of 10 to 100.

Recently, similar cluster methods have been proposed to reduce the critical slowing down for gauge theories [4,5]. The resulting dynamics, based on the percolation of random surfaces in three-dimensional (3D) Z_2 lattice gauge theory, was shown to have a dynamic critical exponent of $z_{\rm RS}=0.73\pm0.15$ [4], nearly equal to the Swendsen-Wang exponent for the 3D Ising model $z_{\rm SW}=0.75\pm0.01$ [1].

In this paper we consider the random surface dynamics at the finite-temperature transition in lattice gauge theory. There are several reasons that make this a natural next step. Simulations of pure glue QCD at finite temperature are already on large enough lattices to see substantial critical slowing down at the finite-temperature transition. More importantly, we believe that the origins of critical slowing down may be simpler at the finite-temperature fixed point relative to the zero-temperature fixed point [6]. This is due to the plausible conjecture that the $d+1$ finite-temperature phase transition is driven by the Z_N degrees of freedom in the center of the SU(N) gauge group, with the Polyakov loop order parameter coupled in an effective d-dimensional Z_N clock model, which is of course equivalent to the Potts model in the cases of most interest—Z_2 for SU(2) Yang-Mills theory or Z_3 for SU(3) QCD. Thus the finite-temperature Z_3 critical dynamics may itself have the essential modes necessary to understand and cure critical slowing down in finite-temperature QCD [7].

Additional support for this picture can be derived from testing our *conjecture* that the dynamic universality class for the $(d+1)$-dimensional gauge theories at the finite-temperature transition are the same as the corresponding bulk transition of a d-dimensional spin model. In particular, we have qualitative as well as numerical evidence that the dynamics critical exponent for $(2+1)$-dimensional Z_2 and Z_3 gauge theories (logarithmic or $z_{\rm RS}<0.3\pm0.1$ and 0.53 ± 0.03, respectively) are consistent with the values for the two-dimensional Z_2 and Z_3 Potts models (logarithmic [8] or $z_{\rm SW}=0.20$–0.27 [9] and 0.55 ± 0.03 [10], respectively) at the finite-temperature transition.

In spite of the physical plausibility of our new dynamic universality conjecture, one must remember that *any* universality in the context of nonlocal models is *a fortiori* surprising and should be submitted to tests. For static universality it is well known that sufficiently strong nonlocal interactions do disrupt universality classes. On the other hand, the surprising picture that is emerging for the nonlocal Swendsen-Wang cluster dynamics is the presence of dynamic universality classes [2]. This paper suggests a nontrivial extension of this emerging picture to include a universality relationship between cluster and surface dynamics analogous to the static Svetitsky-Yaffe [6] conjecture for local statics.

II. RANDOM SURFACE DYNAMICS AT FINITE TEMPERATURE

Although there is a natural generalization of Swendsen-Wang [1] dynamics for discrete spin models to

the case of discrete gauge models [4,5], the generalization exposes contrasting features: The action for a spin model is defined on bonds while the action for a gauge model is defined on plaquettes; the correlation function for a spin model is defined between points encircling lines while the correlation function for a gauge model is defined on loops encircling surfaces; and presumably the mechanism for accelerating the dynamics for spin models is related to the divergence of the connectedness length for the bond percolation cluster accelerating the dynamics for gauge models is related to the divergence of spanning surfaces for plaquette percolation.

Nonetheless one can in effect interpolate between the gauge model and its corresponding one-dimensional lower spin model by going to finite temperature. According to the conjecture of Svetitsky and Yaffe [6], the gauge model at its deconfining phase-transition point (if the transition is continuous) is universal to a spin model with the spin value taken from the center of the original gauge group. This conjecture has been supported by many Monte Carlo simulations with very few exceptions [11,12]. The conjecture in its original form was only proposed for static properties. Here we argue that, in fact, the conjecture of Svetitsky and Yaffe remains true for the particular kind of dynamics we are considering. In particular, we conjecture that the dynamic critical exponents z_{RS} for the random surface dynamics [4,5] for the $(2+1)$-dimensional Z_2 and Z_3 gauge theories at the deconfining phase-transition points are the same as the exponent z_{SW} for the Swendsen-Wang dynamics for the two-dimensional Ising and 3-state Potts models:

$$z_{\mathrm{RS}}^{d+1}=z_{\mathrm{SW}}^{d} . \tag{1}$$

First we give qualitative arguments which leads to the above conjecture. Then we present the numerical results to support the universality conjecture. Also we present data for static scaling results so that the consistency of our data with the static Svetitsky-Yaffe conjecture is verified. Finally, we comment on extensions to models with other gauge groups and to models in four dimensions.

III. QUALITATIVE ARGUMENT

We begin by presenting a plausibility argument for our dynamics universality conjecture. First to simplify the discussion, we consider the example of pure random (or Bernoulli) plaquette percolation on an infinite cubic lattice [13]. There the relevant correlation function is defined for a loop Γ, in a fixed percolated plaquette configuration, as

$$W(\Gamma)=\begin{cases}1 & \text{if } \Gamma=\partial S , \\ 0 & \text{otherwise} ,\end{cases} \tag{2}$$

where S is an unbroken surface made of percolated plaquettes and ∂S is the boundary of S. Analogous to the confinement-deconfinement phase transition, the behavior of $\langle W(\Gamma)\rangle$ ($\langle\cdots\rangle$ stands for ensemble average) is characterized by

$$\langle W(\Gamma)\rangle=\begin{cases}\exp[-\text{area}(\Gamma)] & \text{if } p_s<p_s^* \quad \text{(confined phase)} , \\ \exp[-\text{perimeter}(\Gamma)] & \text{if } p_s>p_s^* \quad \text{(deconfined phase)} ,\end{cases} \tag{3}$$

where p_s and p_s^* are plaquette percolation probability and critical plaquette percolation probability, respectively. Now we imagine that one of the directions (call it the time direction) becomes finite and periodic. Then a new kind of correlation function can be defined for loops $\Omega_1=\Omega(x_1)$ and $\Omega_2=\Omega(x_2)$, which wrap around the time direction through the periodic boundary at fixed spatial positions x_1 and x_2:

$$C_P(x_1,x_2)=\begin{cases}1 & \text{if } \Omega_1+\Omega_2=\partial S , \\ 0 & \text{otherwise} .\end{cases} \tag{4}$$

The asymptotic behavior of $C_P(x_1,x_2)$ as the plaquette probability p_s is varied may signal a new "finite-temperature" phase transition distinct from the "zero-temperature" one on the infinite cubic lattice. It is plausible that this new phase transition is characterized by

$$\langle C_P(x_1,x_2)\rangle \overset{|x_1-x_2|\to\infty}{\longrightarrow} \begin{cases}0 & \text{(confined phase)} , \\ \text{const}\neq 0 & \text{(deconfined phase)} ,\end{cases} \tag{5}$$

where $|x_1-x_2|$ stands for the distance between Ω_1 and Ω_2. Equation (5) is certainly consistent with Eq. (3), since $\Omega_1+\Omega_2$ is a special case of Γ with a finite perimeter. Notice that the Ω's live on a two-dimensional infinite lattice.

In Eq. (4) we have defined the connectedness function $C_P(x_1,x_2)$ by the condition that curves Ω_1 and Ω_2 be homologous on a percolated surface. The ensemble average $\langle C_P(x_1,x_2)\rangle$ gives the probability that x_1 and x_2 lie in the same 2D percolation cluster for an effective two-dimensional bond percolation problem. To illustrate the concept of connectedness defined by the homology condition, we give an example of connectedness in Fig. 1(a) where $C_P(x_1,x_2)=1$, $C_P(x_2,x_3)=1$ and $C_P(x_1,x_3)=1$ and a less trivial case in Fig. 1(b) where $C_P(x_1,x_2)=0$, $C_P(x_2,x_3)=0$ but $C_P(x_1,x_3)=1$. However, since the crucial property of transitive closure [i.e., $C_P(x_1,x_2)=1$, $C_P(x_2,x_3)=1$ implies $C_P(x_1,x_3)=1$] is never violated, there must be some underlying bond percolation process in 2D defined by the projection from the $(2+1)$-dimensional system. In other words Eq. (4) is equivalent to

$$C_B(x_1,x_2)=\begin{cases}1 & \text{if } x_1+x_2=\partial C , \\ 0 & \text{otherwise} ,\end{cases} \tag{6}$$

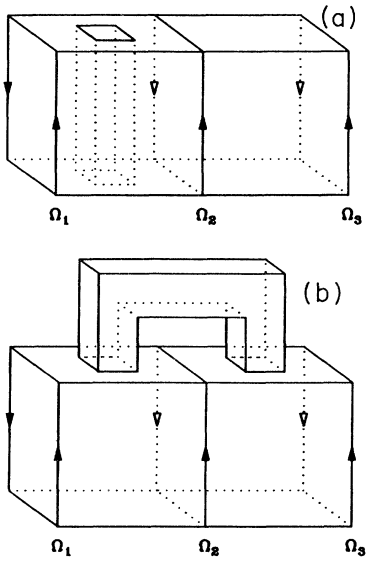

FIG. 1. Examples of the connectedness function for Polyakov loops, Ω_1, Ω_2, and Ω_3 defined by homology on nontrivial topological surfaces with a single handle: (a) a handle that does not break the homology condition between any of the pairs of Polyakov loops; and (b) a handle that breaks the homology between pairs $\Omega_1-\Omega_2$ and $\Omega_2-\Omega_3$ but not $\Omega_1-\Omega_3$.

where C is a continuous curve made of percolated bonds on an infinite two-dimensional square lattice.

Of course we cannot assume that bond percolation is restricted to nearest-neighbor bonds and we cannot determine precisely how the probabilities $p_b(x_1-x_2)$ for bond percolation depend on the plaquette probability p_s. Still once you assume the existence of this mapping, the dynamic universality plaquette percolation on the cubic lattice (with one dimension finite and periodic) and its corresponding bond percolation on a one-dimensional lattice are trivial. Both lattices with their pure Bernoulli percolation "dynamics" have no autocorrelations and thus "universally" is exhibited by both having zero critical slowing down.

Now let us look at the new elements encountered in the nontrivial random surface dynamics of the $(2+1)$-dimensional Z_2 lattice gauge theory. The algorithm that defines the random surface dynamics for the evolution of the gauge field configuration [5] involves percolation only on the nonfrustrated plaquettes, which implies a form of *link correlated plaquette percolation,* $p=1-\exp[-\beta(1+\sigma_P)]$, where σ_P is the field strength associated with a plaquette P. However Eqs. (2)–(5) still hold if the percolation is carried out on the frustration-diluted lattice, with the modification that Eqs. (2) and (4) are now understood as the averages over all the spin configurations compatible with the fixed percolation configurations. Now the question remains whether a similar site correlated bond percolation is induced through Eq. (4). It is not hard to convince oneself that if Ω_1 and Ω_2 have opposite signs, they cannot be the boundary of a closed percolated surface S (i.e., $\Omega_1+\Omega_2=\partial S$ guarantees that Ω_1 and Ω_2 have the same sign). So we expect that a gauge model such as the Z_2 gauge model has a reduction to its corresponding one-dimensional lower spin model, qualitatively similar to the pure Bernoulli percolation case. Dynamic universality would then follow naturally if, as we assume, the effective lower-dimensional spin model is dominated by short-range interactions.

We mention in passing that our universality conjecture is trivial when $N_t=1$ since the spacelike links decouple from the timelike links due to periodicity. The random surface dynamics in $2+1$ dimensions [4,5] gives precisely the Swendsen-Wang dynamics [1] for the space-time plaquettes (i.e., electric term), while the independent space-space plaquettes (i.e., magnetic term) form a noncritical two-dimensional gauge theory. Furthermore, the above picture also emerges in the case of finite N_t as long as the coupling is strong enough such that the plaquette percolation is dominated by the smallest area spanning Ω_1 and Ω_2, or equivalently ignoring the space-space plaquettes in the action. It is also easy to see in this limit that $\beta_{\text{spin}}\approx(\beta_{\text{gauge}})^{N_t}$. Therefore the nearest-neighbor percolation probability is

$$p_b(p_s)=1-\exp[-2\ln^{N_t}(1/\sqrt{1-p_s})]$$

and all other long-range $p_b(p_s)$ vanish.

IV. NUMERICAL METHODS AND RESULTS

The numerical algorithm, used to study universality in the case of $(2+1)$-dimensional Z_2 and Z_3 lattice gauge theories, employs the approach develop by Ben-Av *et al.* [4], which uses the field strengths instead of gauge fields as dynamic variables and the Bianchi identity as a constraint on the dual lattice. On each dual bond (or plaquette) the flux Φ_P is an integer defined mod$N$ so that the field-strength plaquette variable $\sigma_P=\exp(2\pi i\Phi_P/N)$ is an element of Z_N. The Bianchi identity requires flux conservation (mod$N$) at all dual sites. This formulation can be easily translated into an efficient computer algorithm.

(i) Each dual bond is percolated (or turned *on*) with probability: $p=\exp[-\beta(1+\sigma_P)]$.

(ii) A maximal spanning tree is constructed from these *on* bonds. No loops are allowed but the tree can have several disconnected components.

(iii) A random Z_2 or Z_3 group element is assigned to all remaining bonds whose inclusion gives rise to closed loops.

(iv) By traversing the bonds in exactly the reverse order used to constructing the tree, all bonds are determined by the Bianchi identity by requiring the product of group elements at each node to be the identity.

If we were dealing with an infinite cubic lattice, the above steps would be complete. However, on a finite lattice with periodic boundary conditions (always a necessity for the case of finite temperature), there are new nonlocal constraints. These new constraints are related to flux conservation through closed surfaces which do not bound any volume and hence are not a consequence of the local Bianchi identities. For a closed surface the product of all the plaquettes must be positive. In a 3D periodic lattice there are three independent surfaces given by two-tori

parallel to any two lattice axes. To correct for this constraint, we have added one more step to the above numerical algorithm.

(v) Reject any trial configuration which does not satisfy the global constraints.

This rejection is necessary in order to obtain detailed balance on the original lattice with periodic boundary conditions. In general, one might estimate that this constraint will reduce our efficiency by a factor of 8 due to a 50% rejection rate for each two-torus. In fact this is correct in the strong-coupling limit. At the critical point, the reduction is only by about four, which indicates that the time direction is almost frozen. Deep in the deconfined phase, the rejection becomes irrelevant because the number of nonpercolated plaquettes are very few and disconnected and hence do not feel the global structure.

We are also able in each iteration to reconstruct in order of volume operations the gauge fields in terms of field strengths in a maximally fixed gauge. This allows us to calculate the autocorrelation for the Polyakov lines as well as the autocorrelation for the energy.

The relaxation time τ is obtained from the exponential fit to the standard autocorrelation functions, both for the energy and Polyakov line expectation values. For all the Monte Carlo runs a typical iteration number for each lattice size was 5×10^5, with the exception of lattices with $L=128$ which involve half as many iterations. The error in the relaxation time is estimated by dividing the data into ten groups. The error for the dynamic exponents was estimated through the standard propagation of the errors for relaxation times.

A. Static universality

We have also used the random surface algorithm described above to study the static or equilibrium properties of the Z_2 and Z_3 lattice gauge theories at finite temperature in the neighborhood of the deconfining phase-transition point. Again we emphasize the universality between the gauge models and their corresponding spin models conjectured by Svetitsky and Yaffe [6]. Though the Z_2 model have been studied previously, we believe that the Z_3 model has not been studied in as much detail. Also the direct observation of static scaling is important in demonstrating the reliability of our methods. In addition to our fast Monte Carlo algorithm, we use the histogram method of Ferrenberg and Swendsen [14] to generate data away from the critical point. Since the range of validity of the (single) histogram method coincides with the scaling region, we expect this method to be efficient and reliable for our purpose.

Our technique for extracting the critical exponents is the standard finite-size scaling method [15], whereby the singular part of the free energy density is assumed to have the form.

$$f_s(\beta,h,L)=L^{-d}Q(x_t,x_h)\ , \tag{7}$$

with $x_t=(\beta-\beta_c)L^{1/\nu}$, $x_h=hL^{(\beta+\gamma)/\nu}$ and h equal to the external field coupled to the magnetization. We also assume the validity of the hyperscaling relations, such as $\alpha=2-\nu d$, $\gamma=\nu d-2\beta$ and so on, and ignore the irrelevant operators which contribute to the subleading terms. By taking appropriate derivatives of $Q(x_t,x_h)$, we extract convenient combinations of observable. Let us define

$$C_n(\beta)\equiv\left.\frac{\partial^n f_s}{\partial\beta^n}\right|_{h=0}\ , \tag{8}$$

$$\chi_n(\beta)\equiv\left.\frac{\partial^n f_s}{\partial h^n}\right|_{h=0}\ , \tag{9}$$

which in gauge theories are related to the moments of the action and Polyakov expectations, respectively.

Since our primary concern is the universality of the gauge models to their corresponding spin models, we have tried to emphasize this aspect by adapting the following strategy. First we assume the validity of the Svetitsky and Yaffe conjecture and then check the consequences. Namely instead of trying to fit the values of the critical exponents from the data, we fix their values from 2D Ising model for Z_2 gauge theory and 2D 3-state Potts model for Z_3 gauge theory. Then we locate the critical points and check the universality of the scaling functions. For later reference, we note that these exponents [16] are $\nu=1$, $\gamma=\frac{7}{4}$, and $\beta=\frac{1}{8}$ for 2D Ising and $\nu=\frac{5}{6}$, $\gamma=\frac{13}{9}$ and $\beta=\frac{1}{9}$ for 2D 3-state Potts models.

1. *Determination of β_c*

Aided by the scaling relations, it is easy to obtain the relation

$$G(\beta)\equiv\frac{\chi_4(\beta)}{L^d\chi_2^2(\beta)}=\text{const}\times(\beta-\beta_c)L^{1/\nu}+\text{const}\ , \tag{10}$$

which is particularly useful for determining the critical point. Moreover there is another relationship predicted by finite-size scaling [15], which interpolates between the critical point in the thermodynamic limit, $\beta_c\equiv\beta_c(L=\infty)$, and the finite lattice $\beta_c(l)$:

$$\beta_c(L)-\beta_c=\text{const}\times L^{-1/\nu}\ , \tag{11}$$

where $\beta_c(L)$ is the location of the peak in specific heat $C_2(\beta)$ for a system of size L. In general, the advantage of determining β_c in terms of Eq. (10), instead of Eq. (11), is that we do not have to know any details about the model as long as we are close enough to the critical point, while using Eq. (11) requires the knowledge of the exponent ν. If we ignore the subdominant terms, $G(\beta)$ is independent of system size L at $\beta=\beta_c$. So the crossing point corresponds to the critical value we seek. In addition, Eq. (10) tells us how the slope of $G(\beta)$ should vary as a function of L at β_c, even though it does not tell us the absolute values. All the expectations are borne out in Fig. 2. Except for the $L=8$ data, where presumably the subleading terms are still strong, all other data do cross within a very small region. The scatter is used to estimate our errors. The results are

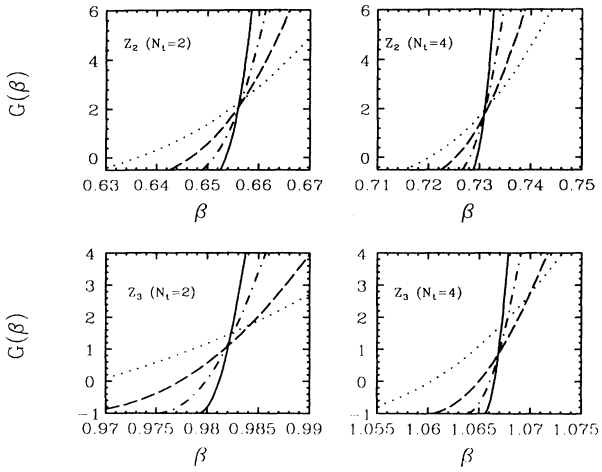

FIG. 2. Plot of $G(\beta)$, defined in Eq. (10). The locations of β at which all the curves cross correspond to the critical point β_c. The dotted, dashed, dot-dashed, and solid curves are the data for $L=8$, 16, 32, and 64, respectively.

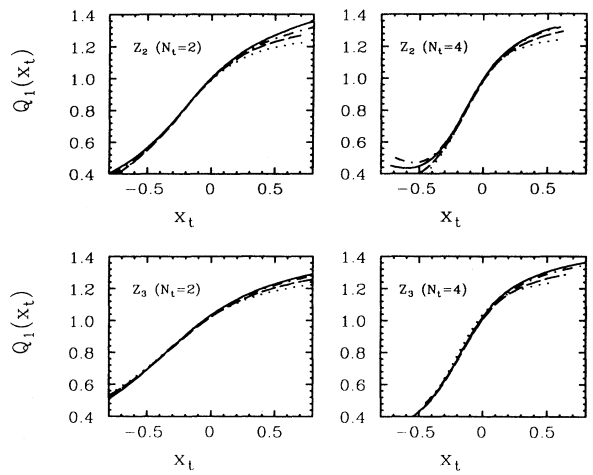

FIG. 3. Plot of $Q_1(x_t)$, defined in Eq. (12) with $x_t=(\beta-\beta_c)L^{1/\nu}$. The β_c's are determined in Fig. 4 and the $1/\nu$'s are taken from the corresponding spin models, explained in the text. The dotted, dashed, dot-dashed, and solid curves are the data for $L=8$, 16, 32, and 64, respectively.

$$\beta_c(Z_2,N_t=2)=0.6562(5)\ ,$$
$$\beta_c(Z_2,N_t=4)=0.7310(5)\ ,$$
$$\beta_c(Z_3,N_t=2)=0.9822(5)\ ,$$
$$\beta_c(Z_3,N_t=4)=1.0668(5)\ .$$

The results for Z_2 are in agreement with Ref. [12]. If we had used Eq. (11) and assumed that ν take the values of their corresponding spin models, we would obtain consistent results with errors twice as big. Notice that the maximum of $C_2(\beta)$ can more easily be found by using the histogram method instead of using many separate Monte Carlo runs to scan in β.

2. *Scaling function*

The expectation value of the Polyakov loop $\Omega(\beta)$, is equal to χ_1, since the regular part contributes nothing to the expectation value of the order parameter. Hence, according to Eq. (7) and the scaling relations, we have the following scaling function for the Polyakov loop expectation value:

$$\Omega(\beta)L^{\beta/\nu}=\left.\frac{\partial Q(x_t,x_h)}{\partial h}\right|_{h=0}\equiv Q_1(x_t)\ . \tag{12}$$

In Fig. 3 we show results in the four different cases (Z_2 and Z_3 for $N_t=2,4$), which as expected support the universality as the system sizes are varied. However, there is another more stringent test of universality [15], which requires that the scaling functions are universal for all the models in the same universality class with the same finite geometry and boundary conditions, up to a rescaling factor for x_t. The interested readers may check for themselves that this requirement is indeed satisfied for the gauge models with different N_t values. A rescaling factor of about 2.0 for $x_t(Z_2,N_t=4)$ will bring $Q_1(Z_2,N_t=4)$ in coincident with $Q_1(Z_2,N_t=2)$, while a rescaling factor of about 1.6 is needed for $x_t(Z_3,N_t=4)$.

3. *Determination of γ/ν*

In principle, after having fitted the scaling functions for $1/\nu$ and β/ν, all other exponents can be determined by using the hyperscaling relations. However, we have made a separate determination of γ/ν to illustrate the power of the histogram method. From the ansatz in Eq. (7), one can deduce the relation

$$\ln\chi_2(\beta_c)=\frac{\gamma}{\nu}\ln L+\text{const.} \tag{13}$$

Figures 4(a) and 4(b) show results for the Z_2 and Z_3 models, respectively. The data in the $\log[\chi(\beta_c)]$ versus $\log(L)$ plots are read off from the curves of $\Omega(\beta)$ and $\chi(\beta)$, generated by the histogram method. The error bars are estimated from the uncertainty of the β_c in each case, which is very sensitively dependent on the precise location of the critical point. Finally, we mention that the expectation that $\alpha=0$ for Z_2 is reproduced by our data.

Before ending this section, a message of caution is in order. The sensitivity for extracting critical exponents by finite scaling depends delicately on precise location of the critical point β_c. A small deviation of β_c from its true value will give very misleading results. It is important to have more than one criterion for determining β_c and to check for consistency of its value before fitting the data to get critical exponents. It is crucial that the histogram method is in fact a very effective method for accomplishing this consistency check.

B. Dynamics universality

We simulated the $(2+1)$-dimensional Z_2 and Z_3 lattice gauge theories by sitting at the critical point for fixed $N_t=2$ or $N_t=4$ and exploring the spatial size dependence for the relaxation time. Figures 5 and 6 summarize our results. For comparison, the Swendsen-Wang relaxation times for the corresponding two-dimensional spin models [or equivalently $(2+1)$-dimensional gauge models with $N_t=1$] are also included.

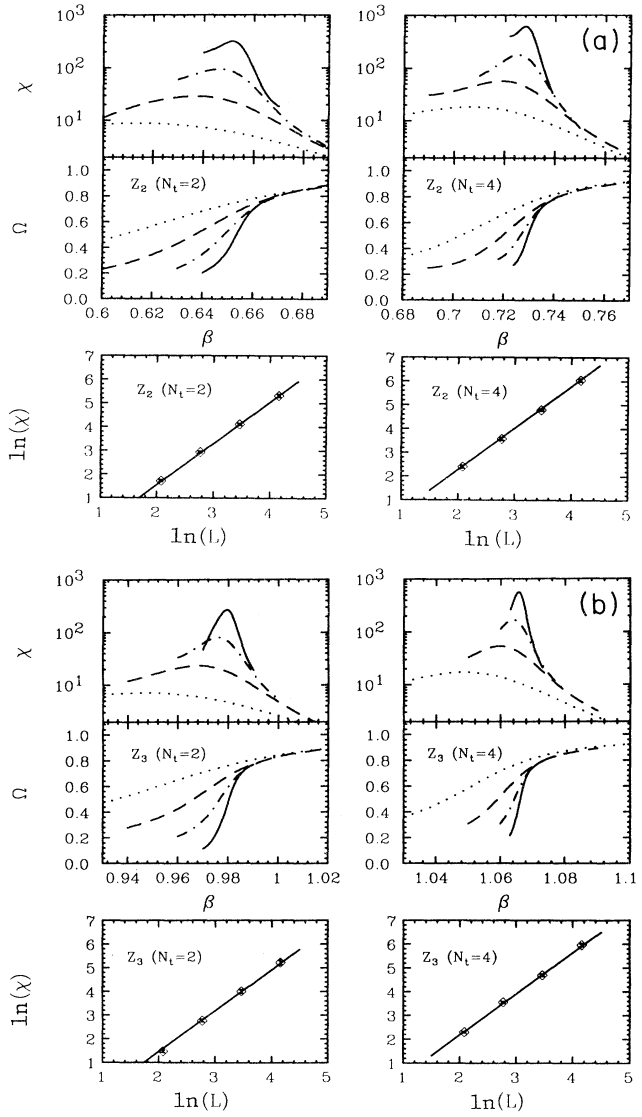

FIG. 4. The upper parts of the figure are the Polyakov loop expectations $\Omega(\beta)$ and susceptibilities $\chi(\beta)$ for Z_2 gauge models with $N_t=2$ and 4. The dotted, dashed, dot-dashed, and solid curves are the data for $L=8$, 16, 32, and 64, respectively. The lower parts of the figure are the log-log (base e natural log) plots according to Eq. (13). The straight lines are the one-parameter linear fits to the data, with the slopes fixed to the corresponding values of γ/ν of 2D Ising model. (b) The data for Z_3 gauge models with the same notation as Fig. 6(a). The straight lines have the slope of 2D 3-state Potts model.

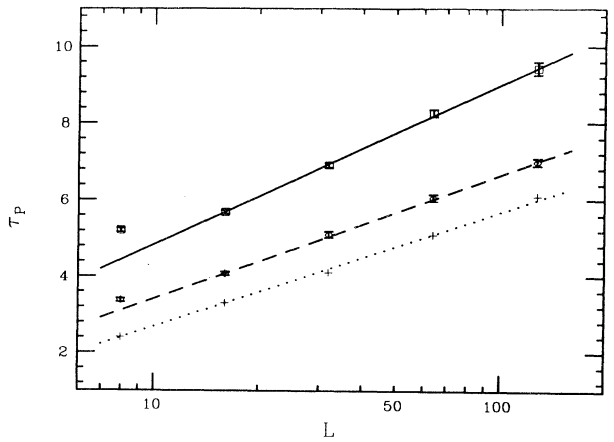

FIG. 5. Semilogarithmic plot for Polyakov line relaxation time τ_P for Z_2 gauge theory versus the spatial size of the system L. The squares are the data for $N_t=4$, diamonds for $N_t=2$, and crosses for $N_t=1$. The lines are meant to guide the eyes. The linear behaviors indicate that τ_P have a logarithmic asymptotics.

In Fig. 5 the linear behavior of the relaxation times for the Polyakov line for different values of N_t versus $\log l$, the logarithm of the linear spatial size, supports the conjecture that the dynamics proposed in [5,4] for $(2+1)$-dimensional Z_2 lattice gauge theory at the deconfining phase-transition point is universal to the Swendsen-Wang dynamics for the 2D Ising model. Autocorrelations for energy gave similar results. In particular, the data is consistent with dynamic-sharing exponents $z_{RS}=0$ and $z_{SW}=0$.

We also studied a log-log plot for the relaxation time versus the spatial size to look for power behavior. Since our lattices are limited to $L\leq 128$, we cannot rule out definitely that the relaxation time for the gauge theory

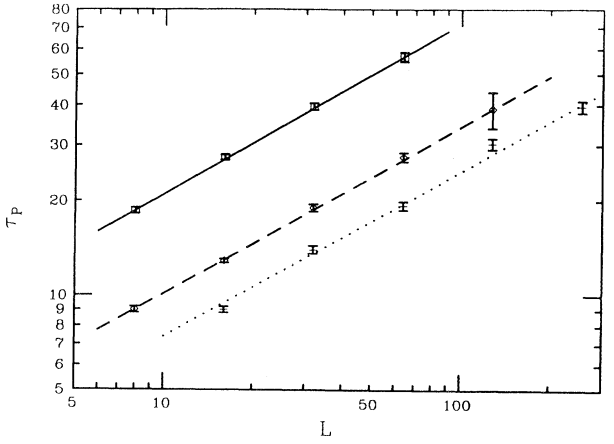

FIG. 6. Log-log plot for Polyakov line relaxation time τ_P for Z_3 gauge theory versus the spatial size of the system L. The squares are the data for $N_t=4$, diamonds for $N_t=2$ and crosses for $N_t=1$. The lines are meant to guide the eyes. Parallel lines indicate τ_P's with the same exponent $z_{RS}=0.53(3)$.

may have a power-law behavior. However, by assuming a power-law behavior, the dynamic exponent appears to decrease with increasing $N_t[z(N_t=1)\approx 0.33$, $z(N_t=2)\approx 0.27$, and $z(N_t=4)\approx 0.22]$. This is very counterintuitive and very unlikely, since the larger N_t is the closer the model is to the crossover to its zero-temperature 3D counterpart, which has a dynamic exponent measured to be $z_{3D}\approx 0.73$ [4,5]. In this sense, our results support the claim [8] that in Swendsen-Wang dynamics for the 2D Ising model the autocorrelation time has logarithmic rather than power-law asymptotics.

Figure 6 shows the results for Z_3 gauge model. The power-law behavior is clearly evident for every N_t value simulated, with the exponent being independent of N_t and estimated to be $z_{RS}=0.54(3)$, compared with the 2D 3-state Potts model $z_{SW}=0.55(3)$ [10].

V. CONCLUSION

Thus far we have considered only the models in 2+1 dimensions with gauge groups Z_2 and Z_3. Since the definitions for correlation functions in Eqs. (1)–(4) do not depend explicitly on the dimensionality, we expect that dynamic universality will also hold between the (3+1)-dimensional Z_2 gauge theory and 3D Ising model. Unfortunately, this point cannot be easily checked numerically since at present we are unable to find an efficient algorithm for finding random surfaces in 4D. Note that in this case the dual problem is also a genuine surface problem. The problem in the (3+1)-dimensional Z_3 model is also difficult since the corresponding spin model, the 3D 3-state Potts model, does not have continuous phase transitions [16], the universality argument cannot be used here. For other gauge groups a useful embedding of the percolation variables into the gauge group has not yet been found, so the formulation of the random surface dynamics is not clear.

Finally, we emphasize that the dynamic universality advocated here has only been discussed for the special nonlocal dynamics proposed in Refs. [4] and [5]. For example, it is not obvious that the heat bath dynamics for (2+1)-dimensional gauge theory at the deconfining phase-transition point is in the same dynamic universality class as the heat bath dynamics for the 2D Ising model. Numerical simulations should be performed to investigate universality. In fact in a heat bath algorithm each link only feels its neighbors, and not the full Polyakov line, so universality appears less compelling to us.

A special feature of the finite-temperature transition is evident in the arguments that map the gauge model into the lower-dimensional spin model. Namely there is a separation of variables between the spatial gauge potentials [$\mathbf{A}(x)$ or the magnetic plaquettes] and the temporal gauge potential [$A_0(x)$ or the electric plaquettes]. By integrating out the spatial potentials at strong coupling, the effective Potts model can be understood as an approximation. Thus in looking for the source of critical slowing down one might regard the "magnetic modes" as fast modes and the "electric modes" as slow.

To test this idea we have performed a Monte Carlo "gedanken" experiment in which the time links are updated many times (N_E) to equilibrate the electric modes followed by a single update of the spatial magnetic modes ($N_B=1$). We observe that by regarding the entire update (many electric hits and one magnetic hit) as single cycle, critical slowing down is drastically reduced the more we rely on magnetic updates ($N_E/N_B\rightarrow\infty$). We feel that additional studies such as this to isolate the slow modes in Monte Carlo algorithms will help both to advance our basic understanding of the dynamic universality classes and to inspire new collective-mode algorithms to circumvent the problem of critical slowing down for large-scale QCD simulations.

ACKNOWLEDGMENTS

It is our pleasure to thank R. Kotiuga and P. Tamayo for many useful discussions. This work was supported in part by DOE Grant No. DE-AE02-86ER40284.

[1] R. Swendsen and J. S. Wang, Phys. Rev. Lett. **58**, 86 (1987); Johannes-Gutenberg Universitat report 1990 (unpublished).
[2] R. C. Brower and P. Tamayo, Phys. Rev. Lett. **62**, 1087 (1989).
[3] U. Wolff, Phys. Rev. Lett. **62**, 361 (1989).
[4] R. Ben-Av, D. Kandel, E. Katznelson, P. G. Lauwers, and S. Solomon, J. Stat. Phys. **58**, 125 (1990).
[5] R. C. Brower and S. Huang, Phys. Rev. D **41**, 708 (1990).
[6] B. Svetitsky and L. Yaffe, Nucl. Phys. **B210** [FS6], 423 (1982).
[7] Technically, in pure SU(3) QCD in 3+1 dimensions, the phase transition may be weakly first order so that there is a large but nondivergent autocorrelation time corresponding to a weaker form of critical slowing down. See F. Brown *et al.*, Phys. Rev. Lett. **61**, 2058 (1988); M. Fukugita, M. Okawa, and A. Ukawa, *ibid.* **63**, 1768 (1989).
[8] D. W. Heermann and A. N. Burkitt, Physica **A162**, 210 (1990).
[9] U. Wolff, Phys. Lett. B **228**, 379 (1989).
[10] X. J. Li and A. D. Sokal, Phys. Rev. Lett. **63**, 827 (1989).
[11] S. Wansleben, Phys. Lett. **148B**, 461 (1984).
[12] S. Wansleben and J. Zittartz, Nucl. Phys. **B280** [FS18], 108 (1987).
[13] M. Aizenman, J. T. Chayes, L. Chayes, J. Frohlich, and L. Rosso, Commun. Math. Phys. **92**, 19 (1983).
[14] A. M. Ferrenberg and R. H. Swendsen, Phys. Rev. Lett. **61**, 2635 (1988).
[15] M. N. Barber, in *Phase Transition and Critical Phenomena,* edited by C. Domb and J. L. Lebowitz (Academic, New York, 1983), Vol. 8.
[16] F. Y. Wu, Rev. Mod. Phys. **54**, 235 (1982).